Single-nuclei RNA sequencing uncovers non-cell autonomous changes in cerebellar astrocytes and oligodendrocytes that may contribute to Spinocerebellar Ataxia Type 1 (SCA1) pathogenesis

Abbreviated title: Single nuclei RNA sequencing in SCA1

Ella Borgenheimer[1#], Ying Zhang[1,2,3], Marija Cvetanovic[1,2*]

1. Department of Neuroscience, University of Minnesota
2. Institute for Translational Neuroscience, University of Minnesota 2101 6th Street SE, Minneapolis, MN 55455
3. Minnesota Supercomputing Institute, University of Minnesota

Currently at Baylor College of Medicine Graduate School of Biomedical Sciences

*Corresponding Author:

Marija Cvetanovic, Department of Neuroscience, University of Minnesota

2101 6th Street SE, Minneapolis, MN 55455

E-mail: mcvetano@umn.edu

Tel. 612-626-4918

Abstract (112 words)

Spinocerebellar ataxia type 1 (SCA1) is a progressive neurodegenerative disease caused by an abnormal expansion of CAG repeats in the gene *Ataxin1* (*ATXN1*). While mutant ATXN1 is expressed throughout the brain, SCA1 is characterized by severe degeneration of cerebellar Purkinje cells (PCs) and cerebellar gliosis. It is likely that cerebellar microenvironment and in particular glial cells contribute to the Purkinje cell specific vulnerability in SCA1. We have used single nuclei RNA sequencing (snRNA seq) to uncover effects of mutant ATXN1 on PCs gene expression changes as well as non-cell autonomous changes in glial cells transcriptomes in cerebella of *Pcp2-ATXN1[82Q]* mice, a transgenic SCA1 mouse model expressing mutant ATXN1 only in PCs cells

Introduction

Spinocerebellar ataxia type-1 (SCA1) is a rare neurodegenerative disorder caused by CAG repeat expansions in the gene *Ataxin-1* (*ATXN1)*[1]. Repeat expansions of about 39 or more repeats result in expression of a toxic polyglutamine (polyQ) ATXN1 protein [2]. Although ATXN1 is expressed throughout the brain, SCA1 is characterized by progressive degeneration that is most severe in the cerebellar Purkinje cells (PCs), and manifests behaviorally as deficits in motor coordination (i.e. ataxia) [3][4][5][6]. While *Atxn1*-targeting antisense oligonucleotides (ASO) show promise in pre-clinical trials [7], there are currently no disease-modifying treatments available for SCA1 [8].

Severe vulnerability of PCs in SCA1 is likely caused by the combination of cell-autonomous effects of mutant ATXN1 on PCs and the PCs microenvironment, including glial cells such as Bergmann glia. Bergmann glia are special type of astrocytes whose cell bodies reside in Purkinje cell layer surrounding the cell bodies of Purkinje cells while their processes extend into the molecular layer next to PCs dendrites enveloping PCs synapses [9]. We have previously shown that Bergmann glia (BG) undergo gliosis, a process of morphological and gene expression changes, including

increased expression of glial fibrillary acidic protein (GFAP) in patients with SCA1 and in SCA1 mouse models [10][11][12]. Moreover, we have demonstrated that early in disease progression astrogliosis has a beneficial role to delay onset and slow the progression of SCA1 pathogenesis in the *Pcp2-ATXN1[82Q]* line, the PCs specific transgenic mouse model of SCA1 [11]. As in this SCA1 mouse model mutant ATXN1 is expressed only in PCs, Bergmann glia undergo gliosis in a response to PCs dysfunction [13]. Identifying the molecular mechanisms that regulate beneficial early astrocyte response to neuronal dysfunction as well as molecular markers of these beneficial astrocytes is important not only to understanding and treatments for SCA1 but for other neurodegenerative diseases in which astrocytes undergo gliosis. We have also found that Bergmann glia become harmful with disease progression [11]. Thus it is important to understand signaling mechanisms that PCs use to activate Bergmann glia early in disease as well as signaling that cause them to change from beneficial to harmful later in disease.

The cerebellum is comprised of several cell types with diverse morphological, biochemical, and electrophysiological properties. Cerebellar glial cells have distinct gene expression compared to the glial cells in other brain regions [14][15] in healthy brains that is even more differentiated during ageing. Glial responses in neurodegeneration and neuroinflammation have been characterized in the cerebrum, much less is known about cerebellar reactive glia [16][17]. While the bulk RNA sequencing has been useful for determining cerebellum-wide changes in the gene expression in mouse models of SCA1, it precludes the detection of transcriptional changes at the single-cell level and is also confounded by the possible change in the proportion of cell types. To investigate whether there is a change in cell composition and transcriptional changes in SCA1 cerebella we used single nuclei RNA sequencing of cerebella from 12 weeks old *ATXN1[82Q]* mice. We used *Pcp2-ATXN1[82Q]* mice as in this SCA1 mouse model mutant ATXN1 is expressed only in PCs so the DEGs and pathways altered in glial cells, including Bergmann glia, velate astrocytes (VA), and oligodendrocytes (OL) are in response to neuronal dysfunction. We chose 12 weeks of age to capture the early middle stage of disease when mice exhibit motor deficits and PCs dendritic atrophy, but there is no PCs death and

disease is still reversible. We also examined gene expression changes in PCs to confirm previously reported transcriptional alterations and to identify changes that could potentially signal activation in glial cells.

Materials and Methods

Mice

The creation of the *Pcp2-ATXN1[82Q]* mice was previously described [18]. We have backcrossed these mice onto C57BL/6 background for 10 generations. As CAG repeats are unstable and tend to shrink in mice we periodically sequence CAG region to evaluate number of repeats. AT the time of experiments the average number of CAG repeats in our colony was 71. Animal experimentation was approved by Institutional Animal Care and Use Committee (IACUC) of University of Minnesota and was conducted in accordance with the National Institutes of Health's (NIH) Principles of Laboratory Animal Care (86–23, revised 1985), and the American Physiological Society's Guiding Principles in the Use of Animals [19].

Nuclei isolation

Nuclei for RNA sequencing were isolated using detergent mechanical lysis protocol as previously described [20]. Briefly, frozen or fresh whole cerebellum was placed into 1.5mL tube with 500uL pre-chilled detergent lysis buffer [low sucrose buffer (LSB) (sucrose 0.32M, 10 mM HEPES, 5mM CaCl2, 3mM MgAc, 0.1mM EDTA, 1mM DTT) with 0.1% Triton-X] and tissue was homogenized using mechanical homogenizer. 40um strainer was placed over a pre-chilled 50mL tube and pre-wetted with 1ml LSB. 1mL of LSB was added to the tube containing the crude nuclei in the lysis buffer and mixed gently by pipetting (2-3 times). Crude nuclei prep was then passed over the 40uM strainer into the pre-chilled 50mL tube, washed with 1 ml LSB and centrifuged at 3200g for 10 minutes at 4C The pellet was resuspended in 3mL of LSB, gently swirling to remove the pellet from the wall to facilitate the resuspension and left on ice for 2 min. Suspension was transferred to an Oak Ridge tube and nuclei were homogenized in LSB for 15-30s, keeping the sample on ice. Using a serological

pipette, 12.5mL of density sucrose buffer (sucrose 1M, 10 mM HEPES, 3mM MgAc, 1mM DTT) was layered underneath the LSB homogenate, taking care not to create a bubble that disrupts the density layer. Samples were then centrifuge at 3200g for 20 minutes at 4C and pelleted nuclei were resuspended in the resuspension solution (PBS, 0.4 mg/ml BSA, 0.2 U/µl RNAse inhibitor). Nuclei were filtered through a 40um pore-size strainer followed by a 30um and 20um pore-size strainers. Small sample of nuclei was pelleted and added to the slide with VectaShield with DAPI to verify single nuclei isolation under fluorescent microscope. The nuclear suspensions were processed by the Genomic Core at the University of Minnesota using 10X Chromium 3' GEX Capture to Library Preparation (Chromium Next GEM Single Cell 3' Reagent Kits v3.1 with Single Cell 3' v3.1 Gel Beads and Chromium Next GEM Chip G).

Sequencing and analysis

Library quality control was performed using MiSeq system to estimate average numbers of nuclei per donor mouse. Then all nuclei from 6 donors were multiplexed and sequenced on two independent runs on the Illumina NovaSeq platform, using 1 full lane of S4 chip each time. Sequencing depth ranges from ~41,000 to ~120,000 reads per nuclei. Raw, demultiplexed fastq files were analyzed by CellRanger (v5.0.1) using reference genome mm10 (refdata-gex-mm10-2020-A), with the option that allows alignment to un-spliced pre-mRNAs (--include-introns). The resulted gene count table per donor was analyzed with R (v4.1.0) package Seurat (v 4.0.4). If bi-modal distribution was observed for nFeature (number of detected genes) per nuclei for a donor, nuclei composing the lower range peak were excluded from downstream analysis. Cell type identification was accomplished with SingleR (v 1.6.1) using DropViz (PMID: 30096299) Cerebellum MetaCells reference.

For identified cell types of Bergmann Cells, Velate Astrocytes, Granule Neurons, Purkinje Neurons and Oligodendrocytes, edgeR (v 3.34.1) was used to test differential abundance between control and KI donors. For the same identified cell types, scran (v 1.20.1) was used to normalize the single cell

expression matrix, followed by limma-trend (v 3.48.3) to test for differential gene expression. Sample batches were considered as an independent factor in the design matrix of the statistical test (design = ~ genotype + batch). P values were adjusted using Benjamini-Hockberg method. Differential gene expression was determined by an adjusted p values of 0.05. The lists of differentially expressed genes from different cell types were further analyzed for GO term enrichment using ClusterProfiler (v 4.0.5). Visualization of the results was generated using various R packages, including Seurat, ClusterProfiler, enrichplot (v 1.12.2), and ggplot2 (v 3.3.5).

Data availability

All the data from this study are available from the authors.

Results

Mutant ATXN1 expression in Purkinje cells does not lead to the significant change in proportions of cerebellar cells

This study aimed to address question how neuronal dysfunction affects glial cells in cerebellar neurodegeneration. To ensure that glial cells are affected solely in the non-cell autonomous manner we have used Purkinje cells specific transgenic mouse model of SCA1, *ATXN1[82Q]* mice [13]. In these mice mutant ATXN1 with 82 polyglutamine repeats is selectively expressed in cerebellar Purkinje cells. We isolated nuclei from the cerebella of 12 weeks-old SCA1 and littermate control mice as previous studies have shown that at this age there is no loss of Purkinje cells but there are significant gene expression changes in the cerebella [21][22]. Previous studies have shown advantages of single nuclei RNAseq compared single cell RNA seq, including preservation of a larger number of cells across multiple subtypes, while minimizing the effects of cell dissociation on gene expression, and enriching for transcripts that are being actively transcribed in vivo [23][24]. Therefore we have performed RNA sequencing on isolated cerebellar individual nuclei that were captured and barcoded (Fig. 1A)[25][26].

We identified a total of 47894 high-quality, snRNAseq profiles. After sequencing, we performed cell typing by classifying nuclei into the cell types using DropViz Cerebellum MetaCells reference [27]. First we wanted to determine whether there is a change in cellular composition of the cerebellum e.g. are numbers of any of the cerebellar cell types increased or decreased in the SCA1 relative to total cell numbers. We calculated the percentage of each cell types by dividing the number of specific cell type by the total number of nuclei.

As expected majority of the nuclei were classified as granule neurons (80.75%). We have focused our analysis on Purkinje cells, Bergmann glia, velate astrocytes and oligodendrocytes. We chose Purkinje cells to compare our data with previously identified SCA1 gene expression changes and identify which ones are specific to Purkinje cells. Bergman glia and velate astrocytes are two types of cerebellar astrocytes residing in the Purkinje cell and granule cell layers respectively [28]. Bergmann glia (BG) have a very intimate contact with Purkinje cells and as such they are the perfectly poised to sense and respond to Purkinje cell dysfunction caused by mutant ATXN1. As velate astrocytes reside further away from Purkinje cells and compared to BG have less direct communication with Purkinje cells, we reasoned they will be less affected. While previous studies have found significant changes in the cerebellar white matter in SCA1 patients and *Pcp2-ATXN1[82Q]* mice little is known about how are oligodendrocytes affected in SCA1 [29][30]

We found no differences in the percentage of cell types between *Pcp2-ATXN1[82Q]* and wild-type mice, indicating there is no obvious change in the cerebellar cell type composition at this stage of disease (Figure 1B). However, using two different analysis methods we found significant numbers of differentially expressed genes (DEGs) in all four cell types (Figure 1C). Remarkably, Bergmann glia and Purkinje cells had a similar number of DEGs despite the fact that mutant ATXN1 was expressed only in Purkinje cells (876 and 798 respectively). This suggests that mutant ATXN1 expression in Purkinje neurons can cause significant transcriptional alterations in Bergmann glia in a non-cell autonomous manner. Both velate astrocytes and oligodendrocytes had a significant number of DEGs (210 and 262 respectively, Figure 1C). These results indicate that ATXN1 induced dysfunction in

Purkinje cells can significantly affect not only nearby Bergmann glia but also velate astrocytes and oligodendrocytes in a non-cell autonomous manner.

Molecular profiling of Purkinje cells

We identified 798 DEGs (p.adj<= 0.05), majority of which were downregulated (76.1%). Hierarchical enriched pathways analysis identified five groups of altered overarching pathways: actin axon cytoplasmic binding, GTPase activator signal transduction, cellular calcium homeostasis transport, cerebellum hindbrain morphogenesis, and intrinsic integral presynaptic density (Figure 2A). GO pathways associated with upregulated genes include synapse ($q = 5.868 \times 10^{-8}$), cell morphogenesis ($q = 2.1 \times 10^{-3}$), glutamatergic and GABA-ergic synapses (q values of 1.2×10^{-5} and 7.6×10^{-4}), cell junction ($q = 1.6 \times 10^{-6}$) and axon guidance ($q = 4.2 \times 10^{-2}$) and SP1 transcription factor $q = 2.5 \times 10^{-5}$). Downregulated genes belonged to many pathways including regulation of ion transport ($q = 1.2 \times 10^{-5}$), calcium transport ($q = 1.3 \times 10^{-4}$), dopaminergic synapse ($q = 3.78\ 10^{-4}$) and spinocerebellar ataxia ($q = 3.9 \times 10^{-6}$).

Previous studies used weighted Gene Coexpression Network Analysis of the cerebellar expression data from *Pcp2-ATXN1[82Q]* mice to identify Magenta Module gene network as a network that significantly correlated with disease and has an expression profile correlating with disease progression in Purkinje cells [31]. Thus the Magenta Module is thought to provide a signature of suppressed transcriptional programs reflecting disease progression in Purkinje cells. We first wanted to examine which of the Magenta Module genes are changed in Purkinje cells in our single nuclei gene expression analysis. Out of 342 magenta genes Allen brain atlas suggested that 94 (27%) are PC enriched, 175 (51%) PC exclusive and 31 (9%) belonging to multiple cells lines [31]. In previous studies not all of the Magenta Module genes were found to be significantly altered at 12 weeks in *Pcp2-ATXN1[82]* mice. Indeed we found that in our data 171 (50%) of Magenta Module genes are altered at 12 weeks of age in *Pcp2-ATXN1[82]* mice. Of those 85 were altered only in PCs (49%) (Figure 2B), 74 (43%) were changed in two or more cell types (Figure 2C).

Most intriguing were 14 (8%) genes that were changed in all four cell types (Figure 2D). Among those genes were the four hub Magenta Module genes *Rgs8*, *Inpp5a*, *Homer 3* and *Dner*. Pathway analysis with KEGG implicated glutamatergic synapse as the most significant pathway (q value of 1.507 $X10^{-4}$), and GO identified regulation of postsynaptic calcium and negative regulation of neuronal death as most significant pathways (q values of 4.2 and 2.2 X 10^{-2}) (Supplementary Figure 1).

Molecular profiling points to disruptions of multiple pathways in Bergmann glia

We identified 876 DEGs (p.adj <= 0.05) in Bergmann glia. Out of these 27% were downregulated and 73% upregulated (Figure 3A). Among the upregulated genes were astrocyte markers glial fibrillary acidic protein (GFAP) and aldehyde dehydrogenase1 (Aldh1a1). Intriguingly, expression of *S100b* was decreased in Bergmann glia (Figure 3B). These changes may indicate reactive gliosis in response to PCs dysfunction.

Hierarchical enriched pathways analysis identified five groups of altered overarching pathways: apical actin cytoskeleton cell, activity localization binding diffusion trapping, axon cytosol bouton terminus, integral transporter channel complex, and asymmetric density synapse neuron (Figure 3C). These overarching pathways include many biological pathways important to function of Bergmann glia such as protein serine/threonine kinase activity, regulation of membrane potential (critical for potassium removal from synapses), GABA−ergic synapse and glutamate receptor binding (critical for sensing neuronal activity), basement membrane, regulation of mitochondrial membrane and permeability apoptotic mitochondrial changes (mitochondrial function), actin cytoskeleton, calcium−dependent protein kinase (calcium being the main regulator of astrocytic function) (Figure 3C). Using a more stringent criteria (p.adj <= 0.01) we found 50 upregulated and 93 downregulated genes (Figure 3D-E). We also found significant changes in the expression of genes involved in BG roles that are key for PC neuronal function (Figure 3F). Expression of *Kcnj10*, encoding the potassium inward rectifier Kir4.1 is decreased in BG at this stage of disease. Previous studies have found that reduced expression of Kcnj10 is sufficient to cause PC dysfunction and ataxia in mice [32]. Moreover expression of *Solute*

carrier family 1 Member 3 (Slc1a3) that encodes for the glutamate transporter Glast that is key to remove synaptic glutamate is also decreased in BG [33]. Intriguingly, expression of *Slc8a1* encoding for the Sodium/Calcium Exchanger 1 (NCX1) a low affinity, high capacitance calcium antiporter membrane protein that functions to regulate intracellular calcium is increased.

Expression of astrocytic synapse-regulating genes show divergent changes. Thrombospondin 1 (Thbs1) that induces formation of silent synapses, glypicans (Gpc6) that regulate synapses and chordin-like 1 (Chrdl1) that regulate synapse maturation [34] did no show differential expression in SCA1 cerebella. However expression of secreted protein acidic and rich in cysteine like 1 (SPARCL1) that directly promotes excitatory synapse formation is reduced while expression of SPARC that antagonizes SPARCL1 is increased. These changes in expression create a decrease in *Sparcl1*/*Sparc* ratio that favors synapse inhibition and likely contributes to decreased number of excitatory VGLUT2 synapses on PCs seen at this stage of disease [11].

Gjb6 and Gja1 encoding for gap junction proteins connexin 30 and 43 regulate astrocyte communication. Expression of *Gjb6* is increased and expression of *Gja1* is decreased in reactive human and mouse astrocytes [35][36]. Expression of both *Gjb6* and *Gja1* is increased in SCA1 BGs, as is the expression of *Aquaporin4* (*Aqp4*) that regulates water homeostasis [37] .

Expression of several trophic factors including fibroblast growth factor (*FGF) 12*, *FGF 14* and *Platelet Derived Growth Factor D (PDGFD)* is also increased in BG at this stage implicating neurosupportive role of BG in SCA1.

BG express calcium permeable AMPA glutamate receptors GLUA1 and GLUA4 (encoded by *Gria1* and *Gria4*) that are important for BG morphology and function of PCs [38]. We have found increased expression of both *Gria1* and *Gria4* in BG from *Pcp2-ATXN1[82Q]* cerebella indicating that their ability to respond to released glutamate may be increased, and as a consequence their calcium influx as well may be increased. We also found a large decrease in the expression of inositol tri phosphate receptor 1 (IP3R1), receptor on the ER that upon binding IP3 binding leads to the calcium influx into cytosol [39], that may be compensatory for the increased expression of calcium permeable AMPA receptors

Importantly, previous studies have found that PC regulate BG character via Sonic hedgehog (Shh) signaling [40]. Expression of Shh receptor *Patched 2* (*Ptchd2*) is decreased in BG in *Pcp2-ATXN1[82Q]* cerebella indicating one critical way in which PC-BG is impacted in SCA1. Additionally expression of downstream transcriptional activator *Gli1* is also decreased, while expression of *Gli3* transcriptional repressor is increased, further supporting dysfunctional Shh PC-BG signaling in SCA1.

Expression of proinflammatory and stress induced transcriptional factors *Foxo1 Jun, NFκB1,* and *Atf7* is also induced in SCA BG while expression of *HopxD*, and *Etv* is reduced, indicating that some of the observed transcriptional changes are mediated by these factors.

Increased expression of genes to promote neurogenesis, gliogenesis and synaptogenesis indicate beneficial compensatory gene expression changes in velate astrocytes

Velate astrocytes reside in granule cell layer and are the only astrocytes in the brain that are largely outnumbered by neurons [41]. Hierarchical enriched pathways analysis identified five groups of altered overarching pathways in SCA1 VA: glial involved projection organization, gliogenesis neurogenesis nervous system, mRNA stability catabolic process, dendritic early spine membrane and asymmetric density synapse calcium−mediated signaling (Figure 4A). There were 210 DEGs (p.adj <= 0.05) in velate astrocytes with majority 79.6% of genes upregulated (Figure 4B).

Most significant GO and KEGG pathways of the downregulated genes are somatodendritic compartment ($q = 2.4 \times 10^{-7}$), glutamatergic synapse ($q = 4.6 \times 10^{-6}$), spinocerebellar ataxia ($q = 1.3 \times 10^{-3}$) and parallel fiber to PC synapse ($q = 2.3 \times 10^{-3}$). Upregulated genes belonged to many developmental GO pathways including neuron projection development, neuron differentiation, neuron development and gliogenesis (q values of 3.2×10^{-8}, 4.2×10^{-7}, 3.6×10^{-7}, and 8.4×10^{-5} respectively).

Among the astrocytic marker genes, *GFAP* and *vimentin* (*vim*) were slightly upregulated indicating gliosis in velate astrocytes (Figure 4C). Expression of *apolipoprotein E* (ApoE) that among other roles contributes to astrocyte activation and BDNF secretion was also increased in velate astrocytes [42][43]. Most of the homeostatic astrocytic genes were not altered with the exception of *Slc1a6*, encoding

glutamate transporter, *Sparcl1*, positive regulator of synapses, *Multiple Epidermal Growth Factor-Like Domains Protein 9* (*Megf9)* and *vascular endothelial growth factor* (*VEGF)*, neurotrophic factor previously shown to ameliorate Purkinje cell pathology in SCA1 [44](Figure 4D). Among the genes encoding astrocyte receptors expression of *Glutamate Metabotropic Receptor 3* (*Grm3*) was upregulated while expression of *IP3R1* and *G Protein Subunit Gamma 13* (*Gng13*) were downregulated (Figure 4E). We found reduced expression of *ETS Variant Transcription Factor 5* (*Etv5*) (Figure 4F).

Increased expression of ApoE indicates immune activation of SCA1 oligodendroglia

Oligodendrocytes (OL) envelop axons with myelin and maintain long-term axonal integrity [45]. Previous studies demonstrated atrophy in white matter already present in pre-manifest carriers of SCA1 mutation [29] as well as in *Pcp2-ATXN1[82Q]* mice [30]. These studies indicated functional changes in oligodendrocytes in SCA1 from the early stages of disease progression. To gain insight into the underlying molecular mechanisms we examined pathways altered in oligodendrocyte nuclei from *Pcp2-ATXN1[82Q]* mice compared to littermate controls. Hierarchical enriched pathways analysis identified five groups of altered overarching pathways: extrinsic cytoplasmic component of plasma membrane, positive regulation of cell projection development, intermediate filament cytoskeleton, endoplasmic reticulum calcium homeostasis and asymmetric synapse and calcium−mediated signaling (Figure 5A). We found 262 DEGs in oligodendrocytes in *ATXN1[82Q]* cerebella, with majority (67.2%) of genes being upregulated (Figure 5B-C).

Pathway analysis of downregulated genes identified glutamatergic synapse ($q = 1.8 \times 10^{-6}$), spinocerebellar ataxia ($q = 10^{-5}$), calcium signaling ($q = 5.42 \times 10^{-5)}$ aldosterone signaling and secretion ($q = 5 \times 10^{-3}$), ion homeostasis ($q = 2.4 \times 10^{-4}$). Among the pathways identified with upregulated genes most significant were intracellular organelle ($q = 3.5 \times 10^{-10)}$, intracellular anatomical structure ($q = 5.5 \times 10^{-9}$), myelin sheath ($q = 1.6 \times 10^{-7}$), movement of cell or subcellular component ($q = 1.8 \times 10^{-5}$) and mRNA processing ($q = 2.7 \times 10^{-5}$).

Among the top ten increased oligodendrocyte genes were *transthyretin* (*Ttr*), *apolipoprotein E* (*ApoE*), *Myelin Oligodendrocyte Glycoprotein* (*Mog*), *claudin11* (*Cldn11*) and two netrin receptors, *Unc5* and *DCC* (Figure 5C). Expression of several oligodendrocyte marker genes including *Transferrin* (*Trf)*, *Mog* and *Cldn11* and *Reticulon 4* (*Rtn4*) was increased (Figure 5D)[45].

We found altered expression of many genes important for oligodendrocyte function (Figure 5E). Among them is increased expression of *Glutamate-Ammonia Ligase* (*Glul*) encoding for glutamine synthetase (GS) a key enzyme that catalyzes the conversion of glutamate to glutamine. Previous studies demostrated that OL glutamine synthetase is important for glutamatergic transmission [46], and that *Glul* expression in OL is increased in chronic pathological conditions including amyotrophic lateral sclerosis (ALS) and multiple sclerosis (MS)[47]. We also found increased expression of *Crystallin Alpha B* (*Cryab*) and *ApoE* in SCA1 OL. Increased *Cryab* and *ApoE* have been associated with protective effects and astrocyte gliosis in other neurodegenerative diseases including Parkinson's disease (PD), Alzheimer's disease (AD) and MS [48][49][50][51][43]. Increased expression of transcriptional factor *JunD*, a functional component of activated protein 1 (AP1) complex that, like NF-κB, regulates many of the inflammatory and immune genes, in SCA1 OL also indicates reactive response in pathogenesis (Figure 5 F)[52].

Discussion

We have employed single nuclei RNA sequencing to investigate transcriptional changes in different cerebellar cell types during the early stages of SCA1 disease progression. We have isolated nuclei from the cerebella of 12 weeks old *Pcp2-ATXN1[82Q]* SCA1 mouse model. In *Pcp2-ATXN1[82Q]* mice mutant ATXN1 is expressed only in the cerebellar Purkinje cells –therefore transcriptional changes observed in glial cells in these mice are caused by PC dysfunction. We have examined changes in two types of cerebellar astrocytes: Bergmann glia that reside next to Purkinje cells and velate astrocytes that reside in granule cell layer. Both of these glial cell types have unique features. While Bergmann glia are radial glia that have a very close relationship with Purkinje cells [53], velate astrocytes have a

unique challenge as the neuron to astrocyte ratio is much larger on granule cell layer than anywhere else in the brain [41]. We also examined gene expression changes in oligodendrocytes as recent studies indicated atrophy of cerebellar white matter in patients with SCA1 and in SCA1 mouse models [29][30].

There are three main findings from our study. First, mutant ATXN1 expression in Purkinje cells causes significant transcriptional alterations in all three cell types in a non-cell autonomous manner. The non-cell autonomous effect of mutant ATXN1 on glial cell transcriptomes is also supported by the type of gene expression changes. Mutant ATXN1 primarily causes downregulation of gene expression in cell autonomous manner in PCs as 76% of genes had reduced expression. This is likely in most part caused by the gain of mutant ATXN1 function resulting in decreased transcription [54]. On the other hand most altered genes were upregulated in Bergmann glia (73%), velate astrocytes (79.6%) and oligodendrocytes (67.2%). We propose that these glial transcriptome changes are in response to Purkinje cell dysfunction instead to their loss, as they precede PC loss by 12 weeks [31].

Second important finding is that proximity to Purkinje cells seems to be an important factor in determining the extent of the transcriptional changes. BG that reside next to Purkinje cells have approximately four times more DEGs than velate astrocytes and oligodendrocytes that reside further away. In fact, Bergmann glia have similar number of DEGs as do Purkinje cells themselves, despite the fact that mutant ATXN1 is expressed only n Purkinje cells. This finding supports the previous evidence of very intimate relationship between PCs and BGs, where BGs soma encircle PCs soma and BGs processes extent into the molecular layer enveloping most of the synapses on PCs dendrites [55]. One of the important communication pathways between PCs and BG is Pcs regulation of BGs character via Sonic hedgehog (Shh) signaling [40]. Intriguingly the expression of Patched 1 (Ptch2) receptor for Shh is decreased in BGs as is the expression of Shh signaling downstream transcription factor Gli1. As previous studies have shown that SHH-Ptch2 communication regulates expression of homeostatic genes *Slc1a3*, *Kcnj10*, and *Aqp4* in Bergmann glia [28] it is possible that decreased Shh signaling

contributes to reduced expression of *Slc1a3* and *Kcnj10* and increased expression of *Aqp4* in SCA1 BG.

Third important finding is that many of the pathways identified in all four cell types regulate synapses, cytoarchitecture, calcium and development. For instance the matricellular proteins, secreted protein acidic and rich in cysteine (SPARC, also known as osteonectin) and SPARC-like 1 (SPARCL1, also known as synaptic cleft 1 (SC1) or Hevin), are produced by astrocytes and regulate excitatory synaptogenesis [56]. While SPARCL1 directly promotes excitatory synapse formation, SPARC specifically antagonizes the synaptogenic activity of SPARCL1. Both proteins are normally expressed in the adult CNS [56], and decreased SPARCL1/SPARC ratio, either due to decreased SPARCL1 or increased SPARC, have been described in reactive human and mouse astrocytes [35][36]. We have found increased expression of Sparcl1 in velate astrocytes indicating that SCA1 VA may help promote excitatory synapse formation in the granule layer. The opposite –increased Sparc and decreased Sparcl1 was found in SCA1 Bergmann glia, indicating reduced excitatory synaptogenic activity in the molecular layer.

Transthyretin (Ttr) is a protein that binds and distributes thyroid hormones in blood and cerebrospinal fluid. While it was previously thought to be produced in the choroid plexus recent studies indicated that it is present in oligodendrocyte precursor cells (OPCs), neurons and astrocytes. Moreover, recent studies found that it plays in regulation of OPCs proliferation and survival [57], described it as regulator of the δ-GABAA-R expression in cerebellar granule neurons [58] and regulator of glycolysis in astrocytes [59]. Intriguingly, we found that *Ttr* was among the most highly upregulated genes in all four examined cell types in SCA1 mice. It will be important to understand what causes *Ttr* upregulation in different cerebellar cell types and which cells are affected by increased *Ttr* in SCA1 cerebella.

Identification of shared pathways, including developmental, ion transport and calcium regulation in SCA1 glia indicate that in response to the PCs dysfunction glial cells undergo similar changes. While some of identified changes may be compensatory allowing for continued cerebellar function, and some

may be pathogenic, it will be important for future studies to identify neuron-glia and glia-glia signaling pathways that mediate these changes.

Acknowledgements:

We acknowledge all the members of Orr and Cvetanovic laboratories for thoughtful discussions and feedback on the study. Work in this study was aided by the Single Cell Services of the University of Minnesota Genomics Center.

Funding:

This work was supported by a National Institute of Health NINDS awards (R01 NS107387 and NS109077 to M.C.)

Author Contributions:

M.C. conceptualized the study. E.B. performed experiments. Y.Z. and M.C. analyzed data. M.C., E.B. and YZ wrote the manuscript.

Conflicts of Interest:

The authors report no conflicts of interest.

Figure legends

Figure 1. Experimental schematics, cell composition and DEGs per cell type in *Pcp2-ATXN1[82Q]* mice. A. Nuclei were isolated from the cerebella of 12 weeks old *Pcp2- ATXN1[82Q]* mice and wild-type littermate controls (N=3 of each). After passing library QC nuclei were sequenced on Illumina NovaSeq platform. **B.** Average percentages of Purkinje cells (PC), Bergman Glia (BG), velate astrocytes (VA), and oligodendrocytes in p*cp2- ATXN1[82Q]* mice and wild-type littermate controls (N=3 of each). **C.** Number of differentially expressed genes in each cell type.

Figure 2. Single nuclei analysis confirms previously identified SCA1 disease associated transcriptional changes in Purkinje cells. A. Enriched pathway analysis for DEG in PCs.

B. Magenta genes that were confirmed in PCs. **C.** Heatplot of magenta genes that are changed in PCs, BG, VA or OL. Red indicates smallest and blue indicates largest q value (False discovery rate (FDR) p value). **D.** Heatplot of Magenta genes that are altered in all four cell types with red indicating smallest and green largest q value.

Figure 3. Mutant ATXN1 causes significant non-cell autonomous gene expression perturbations in SCA1 Bergmann glia. A. Number of upregulated and downregulated genes in SCA1 Bergmann glia. **B**. Log fold change (LogFC) in the expression of astrocyte marker genes. **C.** Enriched pathway analysis for BG. **D.** List of top downregulated genes with q value <0.01. E. List of top upregulated genes with q<0.01. **F.** LogFC of BG genes important for their neuronal support (function), receptors, and transcriptional factors.

Figure 4. Velate astrocytes gene expression changes in SCA1. A. Enriched pathway analysis for VA. **B.** Log FC for all downregulated (top) and upregulated (bottom) VA genes with q<0.05.**C.** Log fold change (LogFC) in the expression of astrocyte marker genes. **D.** Log fold change (LogFC) in the expression of VA genes important for neuronal support (function), receptors, and transcriptional factors.

Figure 5. Gene expression changes in SCA1 oligodendrocytes. A. Enriched pathway analysis for OL. **B.-C.** Log FC for all downregulated (**B**) and upregulated (**C**) OL genes with q<0.05. **D-F.** Log fold change (LogFC) in the expression of oligodendrocyte marker genes (**D**), genes important for OLs function (**E**), and transcriptional factors (**F**).

Supplementary Figure 1. Pathway analysis of Magenta Module genes altered in PCs, BG, VA and OLs in *Pcp2-ATXN1[82Q]* mice.

Literature cited

1. Orr HT, Chung MY, Banfi S, Kwiatkowski TJ Jr, Servadio A, Beaudet AL, McCall AE, Duvick LA, Ranum LP ZH. Expansion of an unstable trinucleotide CAG repeat in spinocerebellar ataxia type 1. Nat Genet. 1993;4:221.

2. Zoghbi HY, Orr HT. Pathogenic mechanisms of a polyglutamine-mediated neurodegenerative disease, Spinocerebellar ataxia type 1. J. Biol. Chem. 2009;284:7425–9.

3. Seidel K, Siswanto S, Brunt ERP, Den Dunnen W, Korf HW, Rüb U. Brain pathology of spinocerebellar ataxias. Acta Neuropathol. 2012;124:1–21.

4. I. K, M. M, T. S-H, M. H, T. K, U. W, et al. Neuropsychological features of patients with spinocerebellar ataxia (SCA) types 1, 2, 3, and 6. Cerebellum. 2010;9:433–42.

5. Zoghbi HY, Pollack MS, Lyons SLA, Ferrell TRE, Daiger SP, Beaudet AL. Spinocerebellar Ataxia : Variable Age of Onset and Linkage to Human Leukocyte Antigen in a Large Kindred. Ann. Neurol. 1988;23:580–4.

6. Koeppen AH. The pathogenesis of spinocerebellar ataxia. The cerebellum. 2005;4:62–73.

7. Friedrich J, Henzler C, Orr HT, Friedrich J, Kordasiewicz HB, Callaghan BO, et al. Antisense oligonucleotide–mediated ataxin-1 reduction prolongs survival in SCA1 mice and reveals disease-associated transcriptome profiles. J. Clin. Investig. 2018;3.

8. Paulson HL, Shakkottai VG, Clark HB, Orr HT. Polyglutamine spinocerebellar ataxias-from genes to potential treatments. Nat. Rev. Neurosci. 2017.

9. Bellamy TC. Interactions between Purkinje neurones and Bergmann glia. The cerebellum. 2006;5:116–26.

10. Cvetanovic M, Ingram M, Orr H, Opal P. Early activation of microglia and astrocytes in mouse models of spinocerebellar ataxia type 1. Neuroscience [Internet]. IBRO; 2015;289:289–99. Available from: http://linkinghub.elsevier.com/retrieve/pii/S0306452215000159

11. Kim JH, Lukowicz A, Qu W, Johnson A, Cvetanovic M. Astroglia contribute to the pathogenesis of spinocerebellar ataxia Type 1 (SCA1) in a biphasic , stage-of-disease specific manner. Glia.

2018;1–16.

12. Rosa J, Hamel K, Sheeler C, Borgenheimer E, Soles A, Ghannoum F, et al. Early stage of Spinocerebellar Ataxia Type 1 (SCA1) progression exhibits region- and cell-specific pathology and is partially ameliorated by Brain Derived Neurotrophic Factor (BDNF). BioRxiv. 2021;1:doi: https://doi.org/10.1101/2021.09.13.460129 ;

13. Burright EN, Clark HB, Servadio a, Matilla T, Feddersen RM, Yunis WS, et al. SCA1 transgenic mice: a model for neurodegeneration caused by an expanded CAG trinucleotide repeat. Cell. 1995;82:937–48.

14. Grabert K, Michoel T, Karavolos MH, Clohisey S, Baillie JK, Stevens MP, et al. Microglial brain region − dependent diversity and selective regional sensitivities to aging. Nat Neurosci. 2016;19:504.

15. Boisvert MM, Erikson GA, Shokhirev MN, Allen NJ. The Aging Astrocyte Transcriptome from Multiple Regions of the Mouse Brain. Cell Rep. [Internet]. ElsevierCompany.; 2018;22:269–85. Available from: https://doi.org/10.1016/j.celrep.2017.12.039

16. Liddelow SA, Barres BA. Reactive Astrocytes: Production, Function, and Therapeutic Potential. Immunity [Internet]. Elsevier Inc.; 2017;46:957–67. Available from: http://dx.doi.org/10.1016/j.immuni.2017.06.006

17. Liddelow SA, Guttenplan KA, Clarke LE, Bennett FC, Bohlen CJ, Schirmer L, et al. Neurotoxic reactive astrocytes are induced by activated microglia. Nature [Internet]. Nature Publishing Group; 2017;541:481–7. Available from: http://dx.doi.org/10.1038/nature21029

18. Watase K, Weeber EJ, Xu B, Antalffy B, Yuva-Paylor L, Hashimoto K, et al. A long CAG repeat in the mouse Sca1 locus replicates SCA1 features and reveals the impact of protein solubility on selective neurodegeneration. Neuron. 2002;34:905–19.

19. National Research Council (US) Committee for the Update of the Guide for the Care and Use of Laboratory Animals. Guide for the Care and Use of Laboratory Animals, 8th edition. 2011.

20. Matson KJE, Sathyamurthy A, Johnson KR, Kelly MC, Kelley MW, Levine AJ. Isolation of adult spinal cord nuclei for massively parallel single-nucleus RNA sequencing. J. Vis. Exp. 2018;2018:1–

12.

21. Ingram M, Wozniak EAL, Duvick L, Zoghbi HY, Henzler C, Orr HT. Cerebellar Transcriptome Profiles of ATXN1 Transgenic Mice Reveal SCA1 Disease Progression and Protection Pathways Article Cerebellar Transcriptome Profiles of ATXN1 Transgenic Mice Reveal SCA1 Disease Progression and Protection Pathways. Neuron [Internet]. Elsevier Inc.; 2016;89:1194–207. Available from: http://dx.doi.org/10.1016/j.neuron.2016.02.011

22. Mellesmoen A, Sheeler C, Ferro A, Rainwater O, Cvetanovic M. Brain derived neurotrophic factor (BDNF) delays onset of pathogenesis in transgenic mouse model of spinocerebellar ataxia type 1 (SCA1). Front. Cell. Neurosci. 2018;

23. Habib N, Avraham-Davidi I, Basu A, Burks T, Shekhar K, Hofree M, et al. Massively parallel single-nucleus RNA-seq with DroNc-seq. Nat. Methods. 2017;14:955–8.

24. Lacar B, Linker SB, Jaeger BN, Krishnaswami S, Barron J, Kelder M, et al. Nuclear RNA-seq of single neurons reveals molecular signatures of activation. Nat. Commun. 2016;7.

25. Klein AM, Mazutis L, Akartuna I, Tallapragada N, Veres A, Li V, et al. Droplet barcoding for single-cell transcriptomics applied to embryonic stem cells. Cell [Internet]. Elsevier Inc.; 2015;161:1187–201. Available from: http://dx.doi.org/10.1016/j.cell.2015.04.044

26. Zilionis R, Nainys J, Veres A, Savova V, Zemmour D, Klein AM, et al. Single-cell barcoding and sequencing using droplet microfluidics. Nat. Protoc. Nature Publishing Group; 2017;12:44–73.

27. Saunders A, Macosko EZ, Wysoker A, Brumbaugh S, Kulp D, Mccarroll SA, et al. Molecular Diversity and Specializations among the Cells of the Adult Mouse Brain Resource Molecular Diversity and Specializations among the Cells of the Adult Mouse Brain. Cell [Internet]. Elsevier Inc.; 2018;174:1015-1030.e16. Available from: https://doi.org/10.1016/j.cell.2018.07.028

28. Farmer WT, Chierzi S, Lui C, Zaelzer C, Jones E V, Bally BP, et al. Neurons diversify astrocytes in the adult brain through sonic hedgehog signaling. Science (80-.). 2016;351.

29. Park YW, Joers JM, Guo B, Hutter D, Bushara K, Adanyeguh IM, et al. Assessment of Cerebral and Cerebellar White Matter Microstructure in Spinocerebellar Ataxias 1, 2, 3, and 6 Using Diffusion

MRI. Front. Neurol. 2020;11:1–13.

30. Liu CJ, Rainwater O, Clark HB, Orr HT, Akkin T. Polarization-sensitive optical coherence tomography reveals gray matter and white matter atrophy in SCA1 mouse models. Neurobiol. Dis. [Internet]. Elsevier; 2018;116:69–77. Available from: https://doi.org/10.1016/j.nbd.2018.05.003

31. Ingram M, Wozniak EAL, Duvick L, Yang R, Bergmann P, Carson R, et al. Cerebellar Transcriptome Profiles of ATXN1 Transgenic Mice Reveal SCA1 Disease Progression and Protection Pathways. Neuron [Internet]. Elsevier Inc.; 2016;89:1194–207. Available from: http://linkinghub.elsevier.com/retrieve/pii/S0896627316001045

32. Djukic B, Kristen B. Casper, Benjamin D. Philpot, Lih-Shen Chin and KDM. Conditional Knock-Out of Kir4.1 Leads to Glial Membrane Depolarization, Inhibition of Potassium and Glutamate Uptake, and Enhanced Short-Term Synaptic Potentiation. J. Neurosci. 2007;27:11354–65.

33. Cvetanovic M. Decreased Expression of Glutamate Transporter GLAST in Bergmann Glia Is Associated with the Loss of Purkinje Neurons in the Spinocerebellar Ataxia Type 1. Cerebellum. 2015;14:8–11.

34. Farhy-Tselnicker, I Boisvert M, Liu H, Dowling C, Erikson G, Blanco-Suarez E, Farhy C, et al. Activity-Dependent Modulation of Synapse-Regulating Genes in Astrocytes. Elife. 2021;10.

35. Barbar L, Jain T, Zimmer M, Kruglikov I, Sadick J, Kalpana K, et al. CD49f is a novel marker of functional and reactive human iPSC- derived astrocytes. Neuron. 2020;107:436–53.

36. Hasel P, Rose IVL, Sadick JS, Kim RD, Liddelow SA. Neuroinflammatory astrocyte subtypes in the mouse brain. Nat. Neurosci. [Internet]. Springer US; 2021;24:1475–87. Available from: http://dx.doi.org/10.1038/s41593-021-00905-6

37. Nagelhus EA, Ottersen OP. Physiological roles of Aquaporin-4 in brain. Physiol. Rev. 2013;93:1543–62.

38. Grosche J, Matyash V, Möller T, Verkhratsky A, Reichenbach A, Kettenmann H. Bergmann Glial AMPA Receptors Are Required for Fine Motor Coordination. Nat. Neurosci. [Internet]. 1999;2:139–43. Available from: http://www.ncbi.nlm.nih.gov/pubmed/10195197

39. Li H, Xie Y, Zhang N, Yu Y, Zhang Q, Ding S. Disruption of IP3R2-mediated Ca2+ signaling pathway in astrocytes ameliorates neuronal death and brain damage while reducing behavioral deficits after focal ischemic stroke. Cell Calcium [Internet]. Elsevier Ltd; 2015;58:565–76. Available from: http://dx.doi.org/10.1016/j.ceca.2015.09.004

40. Farmer WT, Chierzi S, Lui C, Zaelzer C, Jones E V, Bally BP, et al. Neurons diversify astrocytes in the adult brain through sonic hedgehog signaling. Science (80-.). 2016;351:849.

41. Herculano-Houzel S. The glia/neuron ratio: How it varies uniformly across brain structures and species and what that means for brain physiology and evolution. Glia. 2014;62:1377–91.

42. Sen A, Nelson TJ, Alkon DL. ApoE isoforms differentially regulates cleavage and secretion of BDNF. Mol. Brain. Molecular Brain; 2017;10:1–7.

43. Ophir G, Meilin S, Efrati M, Chapman J, Karussis D, Roses A, et al. Human apoE3 but not apoE4 rescues impaired astrocyte activation in apoE null mice. Neurobiol. Dis. 2003;12:56–64.

44. Cvetanovic M, Patel JM, Marti HH, Kini AR, Opal P. Vascular endothelial growth factor ameliorates the ataxic phenotype in a mouse model of spinocerebellar ataxia type 1. Nat Med [Internet]. 2011;17:1445–7. Available from: http://www.ncbi.nlm.nih.gov/entrez/query.fcgi?cmd=Retrieve&db=PubMed&dopt=Citation&list_uids=22001907

45. Bradl M, Lassmann H. Oligodendrocytes: Biology and pathology. Acta Neuropathol. 2010;119:37–53.

46. Xin W, Mironova YA, Shen H, Marino RAM, Waisman A, Lamers WH, et al. Oligodendrocytes Support Neuronal Glutamatergic Transmission via Expression of Glutamine Synthetase. Cell Rep. [Internet]. ElsevierCompany.; 2019;27:2262-2271.e5. Available from: https://doi.org/10.1016/j.celrep.2019.04.094

47. Ben Haim L, Schirmer L, Zulji A, Sabeur K, Tiret B, Ribon M, et al. Evidence for glutamine synthetase function in mouse spinal cord oligodendrocytes. Glia. 2021;69:2812–27.

48. Ousman SS, Tomooka BH, Van Noort JM, Wawrousek EF, O’Conner K, Hafler DA, et al.

Protective and therapeutic role for αB-crystallin in autoimmune demyelination. Nature. 2007;448:474–9.

49. Kuipers HF, Yoon J, Van Horssen J, Han MH, Bollyky PL, Palmer TD, et al. Phosphorylation of αB-crystallin supports reactive astrogliosis in demyelination. Proc. Natl. Acad. Sci. U. S. A. 2017;114:E1745–54.

50. Liu Y, Zhou Q, Tang M, Fu N, Shao W, Zhang S, et al. Upregulation of alphaB-crystallin expression in the substantia nigra of patients with Parkinson's disease. Neurobiol. Aging [Internet]. Elsevier Inc; 2015;36:1686–91. Available from: http://dx.doi.org/10.1016/j.neurobiolaging.2015.01.015

51. D'Agostino M, Scerra G, Cannata Serio M, Caporaso MG, Bonatti S, Renna M. Unconventional secretion of α-Crystallin B requires the Autophagic pathway and is controlled by phosphorylation of its serine 59 residue. Sci. Rep. 2019;9:1–14.

52. Behmoaras J, Bhangal G, Smith J, McDonald K, Mutch B, Lai PC, et al. Jund is a determinant of macrophage activation and is associated with glomerulonephritis susceptibility. Nat. Genet. 2008;40:553–9.

53. Grosche J, Matyash V, Moller T, Verkhratsky A, Reichenbach A, Kettenmann H. Microdomains for neuron-glia interaction: patallel fiber signaling to Bergmann glial cells. Nat Neurosci. 1999;2:139–43.

54. Rousseaux MWC, Tschumperlin T, Lu HC, Lackey EP, Bondar V V., Wan YW, et al. ATXN1-CIC Complex Is the Primary Driver of Cerebellar Pathology in Spinocerebellar Ataxia Type 1 through a Gain-of-Function Mechanism. Neuron. 2018;97:1235-1243.e5.

55. Bell JJL, Lordkipanidze T, Cobb N. Bergmann glial ensheathment of dendritic spines regulates synapse number without affecting spine motility. Neuron Glia Biol. 2010;6:193–200.

56. Kucukdereli H, Allen NJ, Lee AT, Feng A, Ozlu MI, Conatser LM, et al. Control of excitatory CNS synaptogenesis by astrocyte-secreted proteins hevin and SPARC. Proc. Natl. Acad. Sci. U. S. A. 2011;108.

57. Alshehri B, Pagnin M, Lee JY, Petratos S, Richardson SJ. The Role of Transthyretin in Oligodendrocyte Development. Sci. Rep. 2020;10:1–19.

58. Zhou L, Tang X, Li X, Bai Y, Buxbaum JN, Chen G. Identification of transthyretin as a novel interacting partner for the δ subunit of GABA A receptors. PLoS One. 2019;14:12–4.

59. Zawişlak A, Jakimowicz P, McCubrey JA, Rakus D. Neuron-derived transthyretin modulates astrocytic glycolysis in hormone-independent manner. Oncotarget. 2017;8:106625–38.

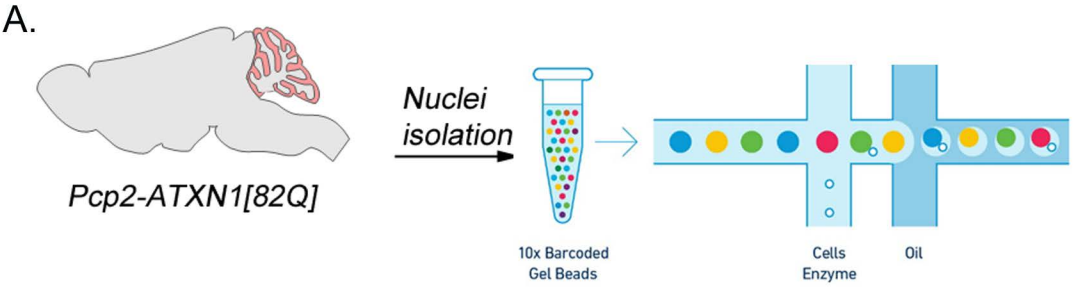
A.
Pcp2-ATXN1[82Q]
Nuclei isolation
10x Barcoded Gel Beads
Cells
Enzyme
Oil

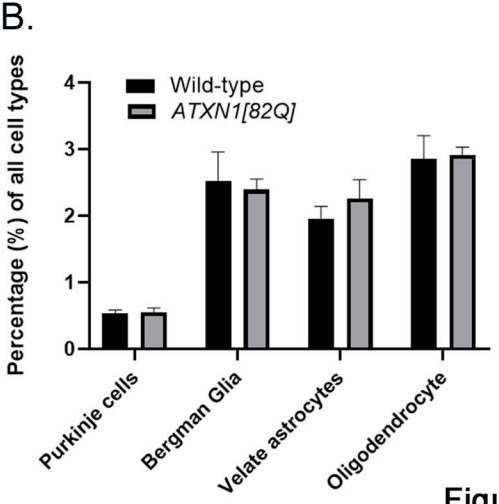
B.
Percentage (%) of all cell types
Wild-type
ATXN1[82Q]
0
1
2
3
4
Purkinje cells
Bergman Glia
Velate astrocytes
Oligodendrocyte

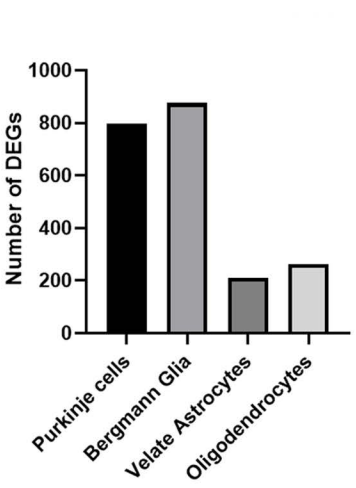
C.
Number of DEGs
0
200
400
600
800
1000
Purkinje cells
Bergmann Glia
Velate Astrocytes
Oligodendrocytes

Figure 1.

A.

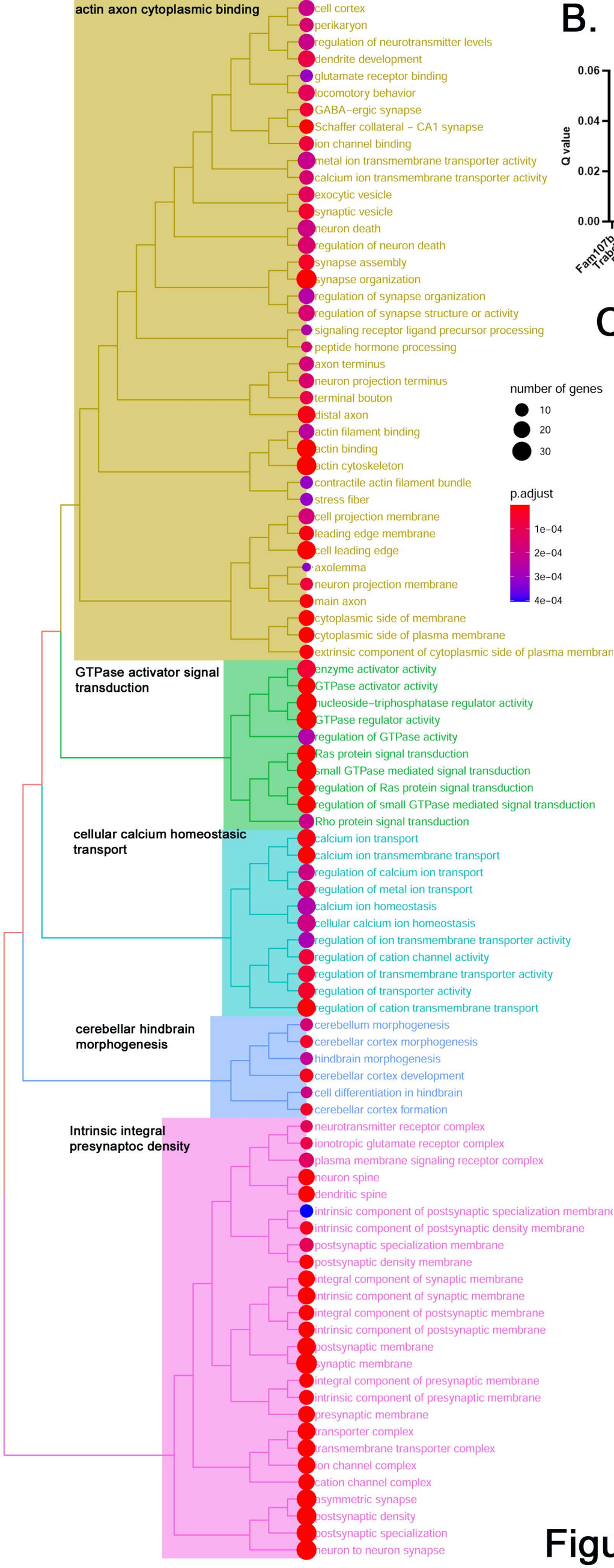

B.

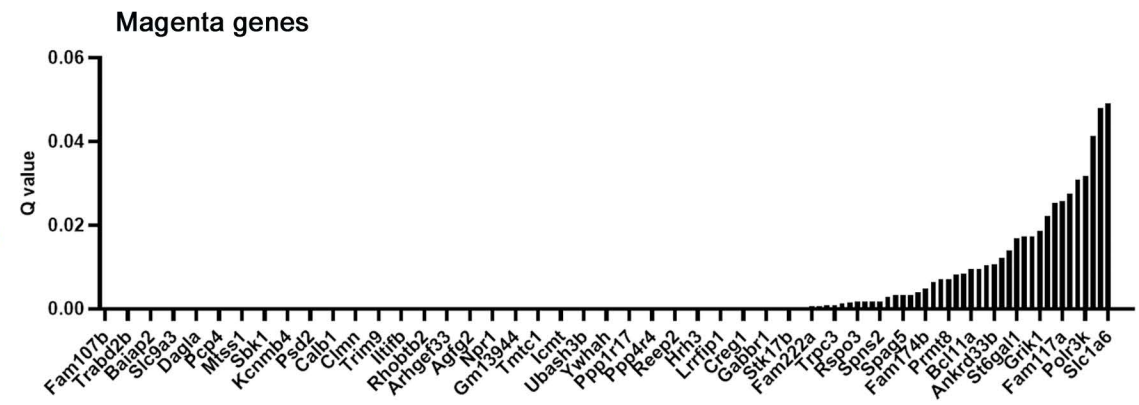

C.

Magenta Genes	BG	VA	PC	OL
Gng13	2.42E-30	3.86E-33	1.25E-09	3.31E-32
Rgs8	1.03E-22	1.89E-12	1.99E-12	1.19E-10
Pcp4	4.44E-22	2.04E-21	2.38E-12	3.93E-27
Itpr1	9.49E-22	1.04E-13	9.80E-09	1.99E-19
Ywhah	7.51E-12	8.62E-06	7.28E-06	7.13E-16
Ppp1r16b	2.64E-11	0.015642578	8.23E-15	0.94234729
Calb1	1.25E-10	8.86E-16	4.40E-09	8.83E-17
Sbk1	8.48E-10	0.007842231	3.09E-10	0.000165644
Shank2	7.50E-09	0.8900877	1.43E-08	0.002409531
Dlg2	3.90E-08	0.510260208	0.027619	0.03586487
Mapk4	1.39E-06	0.300614191	0.04801	0.859967519
Grid2	1.85E-06	0.06074345	7.88E-08	0.691967391
Nsg1	2.03E-06	1.73E-06	0.000601	2.01E-09
Aldoc	1.34621E-05	0.9922944	0.017268	4.55979E-05
Arhgef33	1.66E-05	0.00732529	4.91E-08	7.17E-06
Icmt	4.05E-05	0.017063255	2.39E-06	0.00068911
Ppp1r17	9.56E-05	0.009222756	1.46E-05	7.52E-06
Prkcg	9.96E-05	0.011289547	6.53E-06	0.000157388
Mtss1	0.000125148	0.9553898	1.20E-11	0.633609753
Slc1a6	0.000163476	0.00058137	0.345685	1.44E-06
Npy	0.000377451	0.909222	0.141915	0.706855394
Kctd12	0.00040285	0.184916269	5.43E-05	4.04E-05
Dner	0.000734381	0.002334436	1.17E-05	2.96E-06
Kcng4	0.002024888	0.129670089	0.097437	0.159789023
Hpcal1	0.002250376	0.054266159	5.01E-14	7.57E-05
Ablim2	0.002336696	0.721962542	1.11E-08	0.220624202
Dgkz	0.002698119	0.07141669	6.50E-20	0.247899857
Rnf19b	0.003541673	0.276327914	6.45E-08	0.065813116
Stk17b	0.005069499	0.138739247	0.000338	0.30815562
Plekhd1	0.009085286	0.702758825	1.32E-05	0.046603669
Inpp5a	0.010905223	0.00752449	3.63E-08	0.015802376
Ntng2	0.011671006	0.684878789	0.247225	0.961619953
Lhx1os	0.017803757	0.506903329	5.71E-09	0.467301713
Atp2a3	0.019291157	0.443100752	4.89E-10	0.002806693
Ptprm	0.019560822	0.9793165	1.89E-06	0.932705467
Shisa6	0.019573428	0.443669051	2.19E-07	0.015408383
Cdk16	0.021605841	0.691723075	0.000109	0.665052288
Homer3	0.023096732	0.008522487	7.30E-15	2.49E-05
Prmt8	0.024675765	0.114851594	0.007157	0.120044035
Gprc5b	0.027806883	0.7302208	0.004753	0.623586037
Phactr3	0.030633159	0.8316029	0.002902	0.999751464
Plxdc1	0.036203252	0.499812769	0.003983	0.109829891
Pde5a	0.044410786	0.135339698	0.025291	0.007013958
Reep2	0.045886163	0.302284681	4.64E-05	0.007272081
Inpp4a	0.18213326	0.721962542	0.006494	0.662750009
Cacna1g	0.210664494	0.116025951	2.12E-09	0.015408383
Opn3	0.28593164	0.368567615	0.031845	0.742794238
Lrrfip1	0.390643078	0.546958935	0.000122	0.003274509
Gria3	0.461260555	0.451754592	2.74E-05	0.206517719
Hrh3	0.67509242	0.9981595	6.03E-05	0.739385662
Rmdn3	0.67509242	0.043499957	2.72E-07	0.829068574
Cntnap5b	0.67509242	0.721962542	0.010401	0.766021322
Doc2b	0.700556111	0.552440888	4.27E-09	0.005930736
Id2	0.794114674	0.8961953	1.31E-11	2.12E-05
Grik1	0.868364747	0.080387111	0.018545	0.778020808
Trim9	0.925777713	0.276984233	9.80E-09	0.003079294
Strip2	0.959333514	0.009916515	0.008179	0.031682762
Grid2ip	0.999686246	0.9079816	1.20E-11	0.024548708

D.

Gene	PC	BG	VA	OL
Homer3	7.30E-15	0.023097	0.008522	2.48892E-05
Rgs8	1.99E-12	1.03E-22	1.89E-12	1.19184E-10
Pcp4	2.38E-12	4.44E-22	2.04E-21	3.93415E-27
Gng13	1.25E-09	2.42E-30	3.86E-33	3.30734E-32
Calb1	4.40E-09	1.25E-10	8.86E-16	8.82772E-17
Itpr1	9.80E-09	9.49E-22	1.04E-13	1.99342E-19
Inpp5a	3.63E-08	0.010905	0.007524	0.015802376
Arhgef33	4.91E-08	1.66E-05	0.007325	7.17118E-06
Icmt	2.39E-06	4.05E-05	0.017063	0.00068911
Prkcg	6.53E-06	9.96E-05	0.01129	0.000157388
Ywhah	7.28E-06	7.51E-12	8.62E-06	7.12927E-16
Dner	1.17E-05	0.000734	0.002334	2.96318E-06
Ppp1r17	1.46E-05	9.56E-05	0.009223	7.51993E-06
Nsg1	0.000601	2.03E-06	1.73E-06	2.00972E-09

Figure 2.

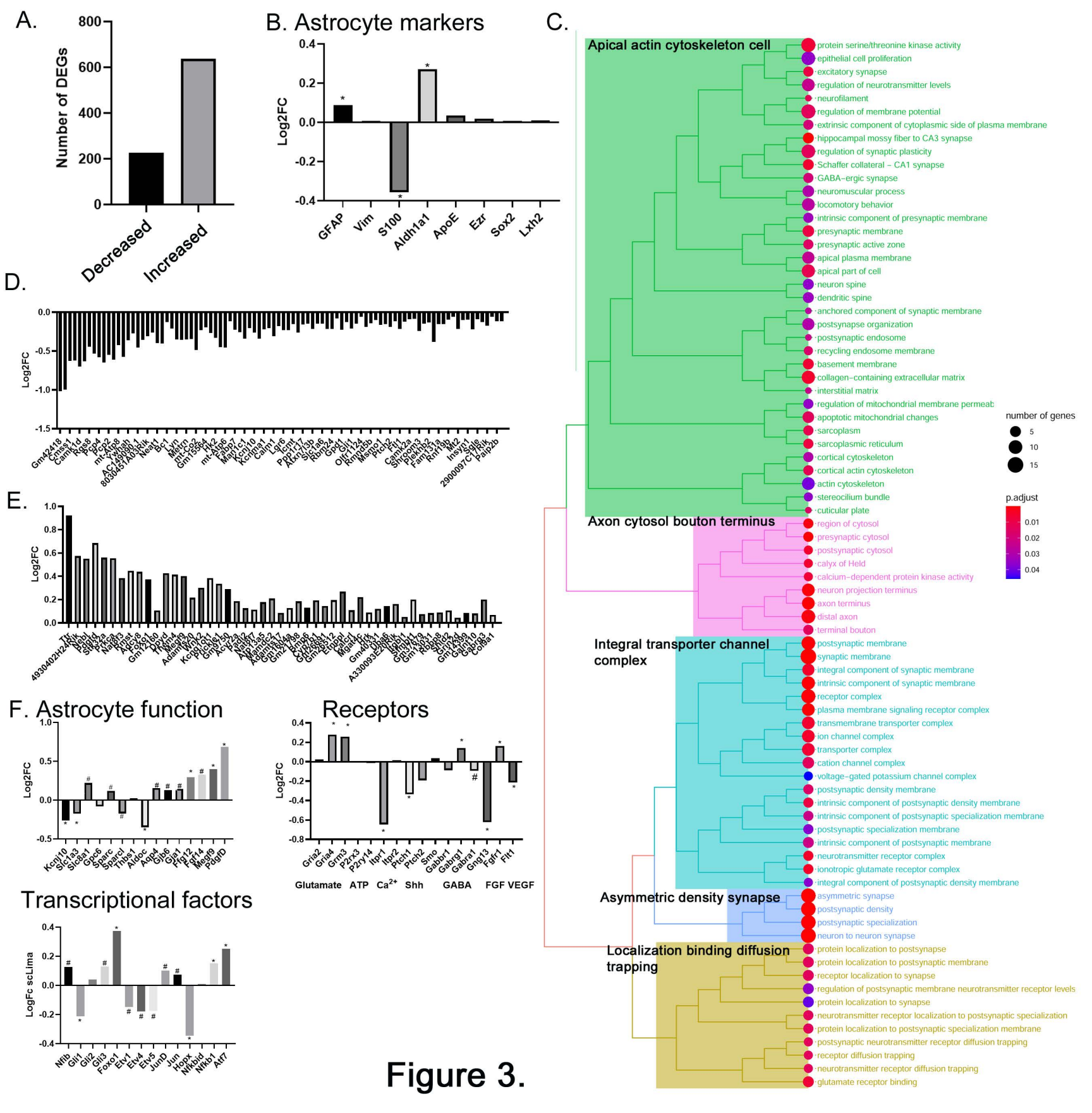
A.
Number of DEGs
800
600
400
200
0
Decreased
Increased
B. Astrocyte markers
Log2FC
0.4
0.2
0.0
-0.2
-0.4
GFAP
Vim
S100
Aldh1a1
ApoE
Ezr
Sox2
Lxh2
C.
Apical actin cytoskeleton cell
protein serine/threonine kinase activity
epithelial cell proliferation
excitatory synapse
regulation of neurotransmitter levels
neurofilament
regulation of membrane potential
extrinsic component of cytoplasmic side of plasma membrane
hippocampal mossy fiber to CA3 synapse
regulation of synaptic plasticity
Schaffer collateral - CA1 synapse
GABA-ergic synapse
neuromuscular process
locomotory behavior
intrinsic component of presynaptic membrane
presynaptic membrane
presynaptic active zone
apical plasma membrane
apical part of cell
neuron spine
dendritic spine
anchored component of synaptic membrane
postsynapse organization
postsynaptic endosome
recycling endosome membrane
basement membrane
collagen-containing extracellular matrix
interstitial matrix
regulation of mitochondrial membrane permeab
apoptotic mitochondrial changes
sarcoplasm
sarcoplasmic reticulum
cortical cytoskeleton
cortical actin cytoskeleton
actin cytoskeleton
stereocilium bundle
cuticular plate
Axon cytosol bouton terminus
region of cytosol
presynaptic cytosol
postsynaptic cytosol
calyx of Held
calcium-dependent protein kinase activity
neuron projection terminus
axon terminus
distal axon
terminal bouton
Integral transporter channel complex
postsynaptic membrane
synaptic membrane
integral component of synaptic membrane
intrinsic component of synaptic membrane
receptor complex
plasma membrane signaling receptor complex
transmembrane transporter complex
ion channel complex
transporter complex
cation channel complex
voltage-gated potassium channel complex
postsynaptic density membrane
intrinsic component of postsynaptic density membrane
intrinsic component of postsynaptic specialization membrane
postsynaptic specialization membrane
intrinsic component of postsynaptic membrane
neurotransmitter receptor complex
ionotropic glutamate receptor complex
integral component of postsynaptic density membrane
Asymmetric density synapse
asymmetric synapse
postsynaptic density
postsynaptic specialization
neuron to neuron synapse
Localization binding diffusion trapping
protein localization to postsynapse
protein localization to postsynaptic membrane
receptor localization to synapse
regulation of postsynaptic membrane neurotransmitter receptor levels
protein localization to synapse
neurotransmitter receptor localization to postsynaptic specialization
protein localization to postsynaptic specialization membrane
postsynaptic neurotransmitter receptor diffusion trapping
receptor diffusion trapping
neurotransmitter receptor diffusion trapping
glutamate receptor binding
number of genes
5
10
15
p.adjust
0.01
0.02
0.03
0.04
D.
Log2FC
0.0
-0.5
-1.0
-1.5
Gm42418
Cmss1
Cam1d
Rgs9
Pcp4
Pcp2
Atp8
mt-Atp8
Ywhah
AC149090.1
8030451A03Rik
Neat1
Bc1
Lyn
Malrn
mt-Co2
Gm15564
Hk2
mt-Atp6
Fabp7
Mapt
Kcnj10
Kcnqa1
Calm1
Lgr6
Lcmt1
Ppp1r17
Atxn1l5b
Slc1a6
Rbm24
Gpd1
Gli1
Olfr1124
Rmpd5b
Msmo1
Ptch2
Fth1
Camk2a
Shroom3
Plekhb2
Fam131a
Rnf19b
Mt2
Insyn1
Sgle
2900097C17Rik
Palp2b
E.
Log2FC
1.0
0.8
0.6
0.4
0.2
0.0
Tr
Hk1
Pebp1
Shbg
Slc22a
Nanp
Ankrd13
Apnat
Kcnk8
Foxo1
Gm12160
Dpp4
Gnc4
Mefv
Adamts20
Wnk2
Kcnq1
Pitpnc1
Gng13
Acvr2a
Aldh1a2
Nalcn
Ag3a5
Adamts2
Adamts17
Gm15418
Bmp6
Chrna6
Gm26551
Gm26532
Etnppl
Mgat4c
Gm40101
Hhk
Gm26656
Slc6a1
Gm10619
Gm10101
Abca8a
Slc16a2
Gm14399
Gabrb3
Col9a1
F. Astrocyte function
Log2FC
1.0
0.5
0.0
-0.5
Kcnj10
Slc1a3
Slc2a1
Gpc6
Sparc
Sparcl
Thbs1
Aldoc
Aqp4
Gjb6
Gja1
Fgf12
Fgf14
Megf9
Pdgfd
Receptors
Log2FC
0.4
0.2
0.0
-0.2
-0.4
-0.6
-0.8
Gria2
Gria4
Grm3
P2rx3
P2ry14
Itpr1
Itpr2
Ptch1
Ptch2
Smo
Gabbr1
Gabrg1
Gabra1
Gng13
Fgfr1
Flt1
Glutamate
ATP
Ca2+
Shh
GABA
FGF
VEGF
Transcriptional factors
LogFc scLima
0.4
0.2
0.0
-0.2
-0.4
Nfib
Gli1
Gli2
Gli3
Foxo1
Etv1
Etv4
Etv5
JunD
Jun
Hoxx
Nfkbid
Nfkb1
Atf7

Figure 3.

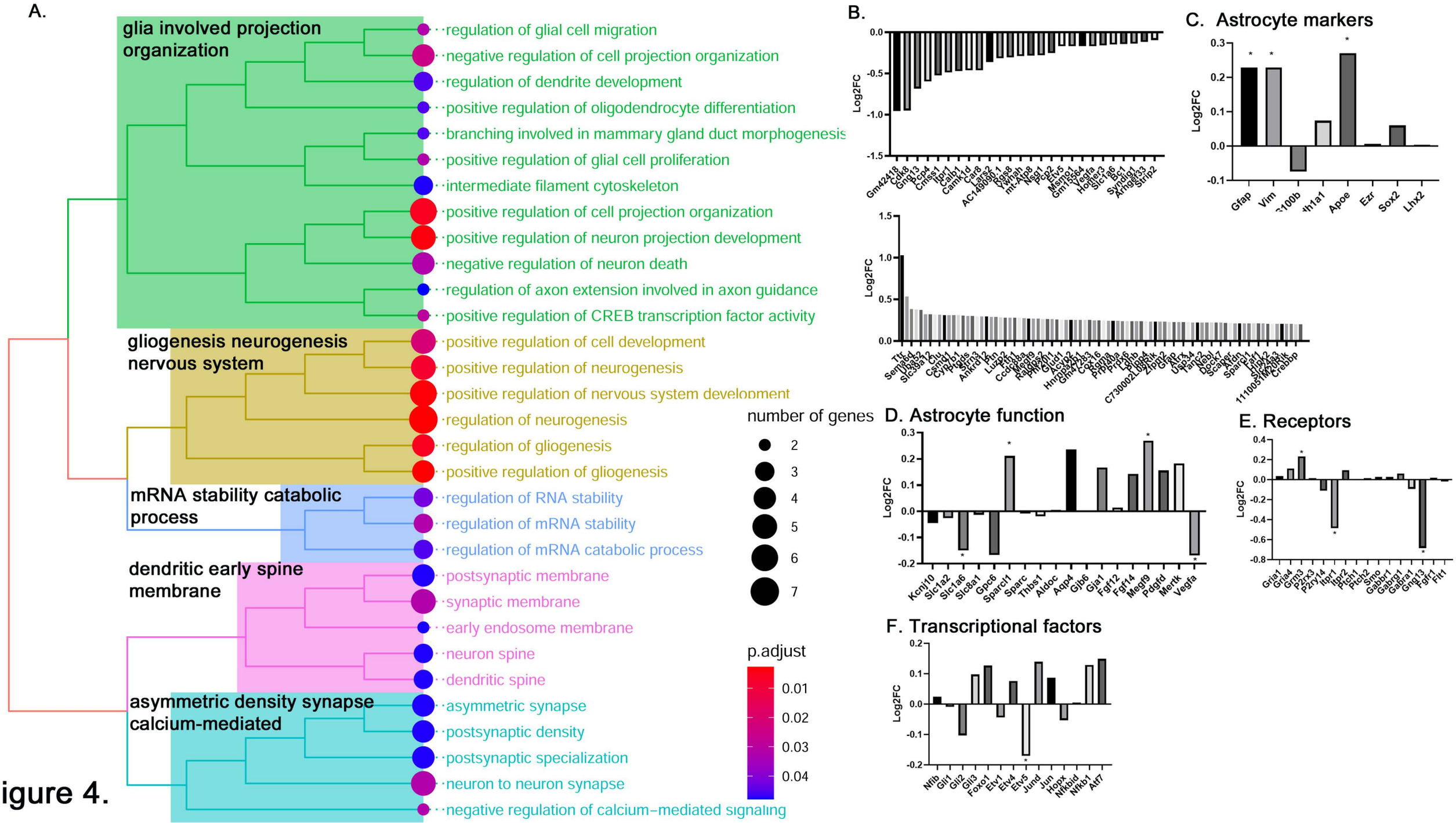
A.
glia involved projection organization
regulation of glial cell migration
negative regulation of cell projection organization
regulation of dendrite development
positive regulation of oligodendrocyte differentiation
branching involved in mammary gland duct morphogenesis
positive regulation of glial cell proliferation
intermediate filament cytoskeleton
positive regulation of cell projection organization
positive regulation of neuron projection development
negative regulation of neuron death
regulation of axon extension involved in axon guidance
positive regulation of CREB transcription factor activity
gliogenesis neurogenesis nervous system
positive regulation of cell development
positive regulation of neurogenesis
positive regulation of nervous system development
regulation of neurogenesis
regulation of gliogenesis
positive regulation of gliogenesis
mRNA stability catabolic process
regulation of RNA stability
regulation of mRNA stability
regulation of mRNA catabolic process
dendritic early spine membrane
postsynaptic membrane
synaptic membrane
early endosome membrane
neuron spine
dendritic spine
asymmetric density synapse calcium-mediated
asymmetric synapse
postsynaptic density
postsynaptic specialization
neuron to neuron synapse
negative regulation of calcium−mediated signaling
number of genes
2
3
4
5
6
7
p.adjust
0.01
0.02
0.03
0.04
B.
Log2FC
Gm42418 Cdk8 Gng13 Pcp4 Cmss1 Tpr1 Calb1 Camk1d Car8 Lars2 AC149090.1 Rgs8 Ywhah mt-Atp8 Nsg1 Pcp2 Etv5 Msmp1 Gm15564 Vegfa Homer3 Slc1a6 Bc1 Syndig1 Arhgef33 Strip2
Ttr Serpina6 Dbx2 Slc39a12 Cu Camq1 Cyp4b1 Tgfbrs Sfrn3 Ankrd12 Pln Luzp2 Ftl1 Ccdc184a Megfg Rab26 Phf24 Glud1 Acyp2 Hnrnpa2b1 Gm42183 Cox16 Rapgn1 Prr14la Prdx6 Lgi1 Lpp4 C730002L08Rik Zfp692 Grap Atf3 Usp54 Tanc2 Nbl1 Dpcd Scaper Atcn1 Sparcl1 Fat1 Hpx2 Slpr3 111005M20Rik Crebbp
C. Astrocyte markers
Gfap Vim S100b Ch1a1 Apoe Ezr Sox2 Lhx2
D. Astrocyte function
Kcnj10 Slc1a2 Slc1a6 Slc8a1 Gpc6 Sparcl1 Sparc Thbs1 Aldoc Aqp4 Gjb6 Gja1 Fgf12 Fgf14 Megf9 Pdgfd Mertk Vegfa
E. Receptors
Gria1 Gria4 Grm3 P2rx3 P2ry14 Itpr1 Itpr2 Ptch1 Ptch2 Smo Gabbr1 Gabrg1 Gabra1 Gnq13 Fgfr1 Flt1
F. Transcriptional factors
Nfib Gli1 Gli2 Gli3 Foxo1 Etv1 Etv4 Etv5 Jund Jun Hopx Nfkbid Nfkb1 Atf7

Figure 4.

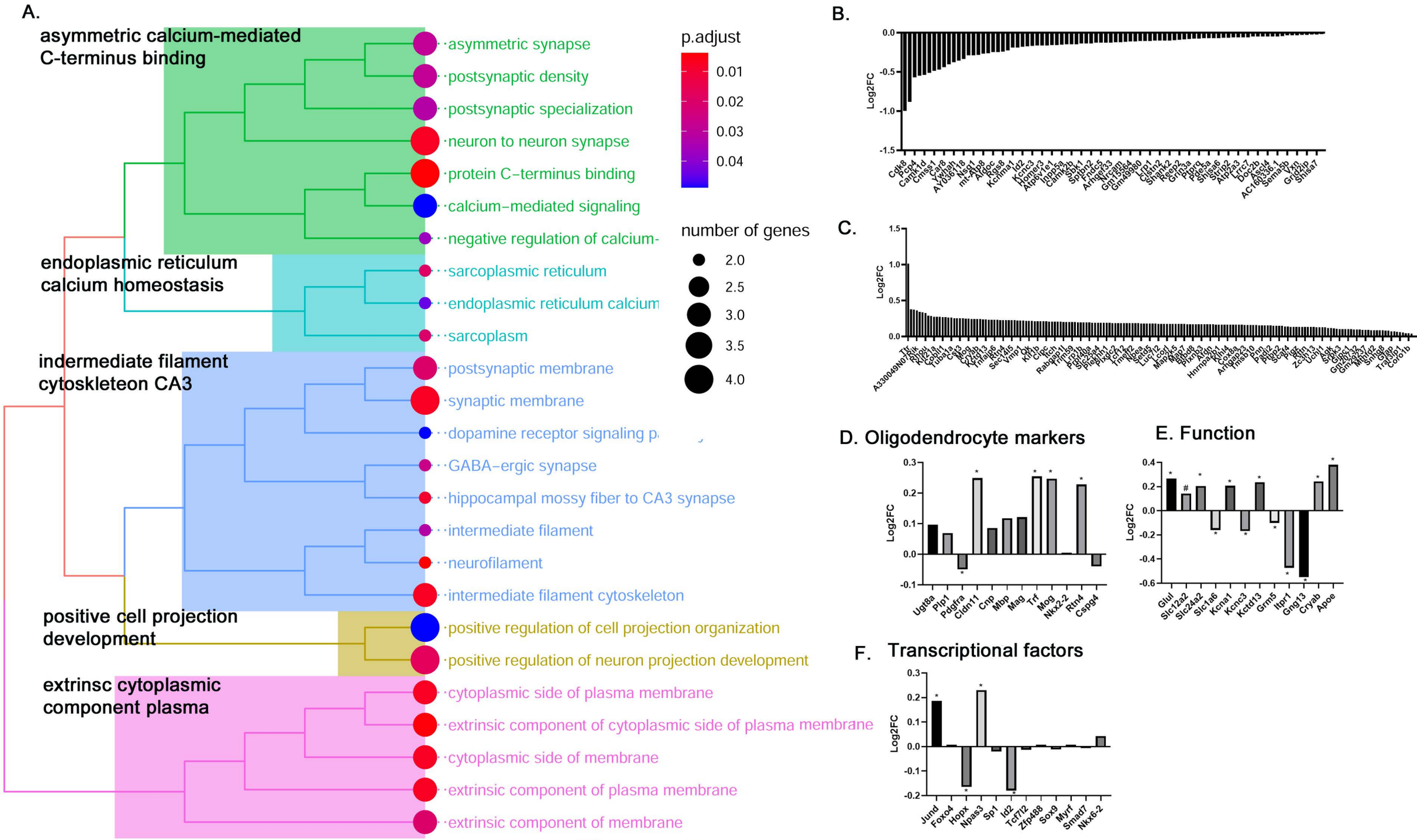
A.
asymmetric calcium-mediated C-terminus binding
endoplasmic reticulum calcium homeostasis
indermediate filament cytoskleteon CA3
positive cell projection development
extrinsc cytoplasmic component plasma
asymmetric synapse
postsynaptic density
postsynaptic specialization
neuron to neuron synapse
protein C-terminus binding
calcium-mediated signaling
negative regulation of calcium-
sarcoplasmic reticulum
endoplasmic reticulum calcium
sarcoplasm
postsynaptic membrane
synaptic membrane
dopamine receptor signaling p
GABA-ergic synapse
hippocampal mossy fiber to CA3 synapse
intermediate filament
neurofilament
intermediate filament cytoskeleton
positive regulation of cell projection organization
positive regulation of neuron projection development
cytoplasmic side of plasma membrane
extrinsic component of cytoplasmic side of plasma membrane
cytoplasmic side of membrane
extrinsic component of plasma membrane
extrinsic component of membrane
p.adjust
0.01
0.02
0.03
0.04
number of genes
2.0
2.5
3.0
3.5
4.0
B.
Log2FC
C.
Log2FC
D. Oligodendrocyte markers
Log2FC
Ugt8a
Plp1
Pdgfra
Cldn11
Cnp
Mbp
Mag
Trf
Mog
Nkx2-2
Rtn4
Cspg4
E. Function
Log2FC
Glul
Slc12a2
Slc24a2
Slc1a6
Kcna1
Kcnc3
Kctd13
Grm5
Itpr1
Gng13
Cryab
Apoe
F. Transcriptional factors
Log2FC
Jund
Foxo4
Hopx
Npas3
Sp1
Id2
Tcf7l2
Zfp488
Sox9
Myrf
Smad7
Nkx6-2

Figure 5.